Structural, Morphological, Optical Properties and Modelling of Ag Doped CuO/ZnO/AZO Solar Cell

Ilhan Candan[1,*], Serap Yigit Gezgin[2], Silan Baturay[1] and Hamdi Sukur Kilic[2,3,4]

[1]*Department of Physics, Faculty of Science, Dicle University, 21280 Diyarbakir, Turkey*

[2]*Department of Physics, Faculty of Science, University of Selcuk, 42031 Selcuklu, Konya, Turkey*

[3]*Directorate of High Technology Research and Application Center, University of Selcuk, 42031 Selcuklu, Konya, Turkey*

[4]*Directorate of Laser-Induced Proton Therapy Application and Research Center, University of Selçuk, 42031 Konya, Turkey*

Abstract: Copper (II) oxide (CuO) has attained significant attention from researchers because of its unique chemical and physical properties. Ag-doped CuO thin films have been produced on the soda glass substrate (SLG) by spin coating technique at different doping ratios. Structural, morphological, and optical properties of thin films produced depending on altered silver ratios have been examined through X-ray diffraction (XRD) spectroscopy, scanning electron microscopy (SEM), and UV-vis absorption spectroscopy, respectively. Band gaps of prepared undoped and 1% Ag-doped CuO thin films have been measured as 1.90eV and 1.63eV, respectively. Ag/undoped CuO and Ag-doped CuO/ZnO/AZO solar cells have been modelled, and their photovoltaic parameters have also been calculated using the SCAPS-1D simulation program. This work aims to investigate the photovoltaic parameters that would improve the efficiency of a solar cell. The effect of Ag atoms on the efficiency of CuO solar cells has been investigated depending on the acceptor density (N_a), the interface defect density (N_t), and the operating temperature. Ag-doped CuO solar cells have shown the highest efficiency for $N_t=10^{10}$ cm^{-3} and N_a=6, 5x10^{16} cm^{-3} values. It has been well observed that as the operating temperature increases, the solar cells' power conversion efficiency decreases. The highest charge generation rates in the undoped and Ag-doped solar cells have been determined as 1.49×10^{22} 1/cm^3.s and 1.51×10^{25} 1/cm^3.s, respectively. All the results, either theoretical or experimental, have been presented in this work and have been compared for a conclusion that has been made in detail.

1. INTRODUCTION

In recent years, copper oxides have been widely used in gas sensors [1], thin film transistors [2], photo-electrochemical cells [3, 4], and cross-point memories [5], including electronic and optoelectronic devices due to their energy band gap values differing from 1.5 to 3eV. CuO-based thin films have very prominent advantages due to their relatively high optical absorption properties, non-toxicity, low production costs, and thermal stabilities [6, 7].

CuO thin films have been produced by using numerous methods such as spray pyrolysis [8], pulsed laser deposition (PLD) [9], sol-gel [10], chemical solution deposition [11], thermal oxidation [12], thermal evaporation [13], chemical vapour deposition [14] and spin coating technique [15]. In

these studies, performed on CuO thin films, effects of various parameters such as annealing methods, deposition temperature, thin film thickness, distance from solution to spray head, solvent properties, and deposition time have been investigated in detail. These parameters have changed the physical properties of thin films obtained, leading researchers to improve (optimise) the characteristics of CuO thin film to be obtained by using different doping ratios. Panah *et al*. [16] have shown that the conductivity of CuO thin films obtained using the sputtering technique increases with titanium (Ti) doping. In addition, in their study [16], they produced solar cells on n-Si, and they found that Ti has significantly changed the short-circuit current value and efficiency of CuO. Basith *et al*. [17] have shown that the energy band gap value and ferromagnetic properties of CuO thin films vary depending on the amount of Fe^{2+} ions dopant. El-Sayed *et al*. [18] have investigated the optical, structural, and photocatalytic properties of Fe and Co-doped CuO thin

*Department of Physics, Faculty of Science, Dicle University, 21280 Diyarbakir, Turkey; E-mail: ilhan.candan@dicle.edu.tr

films obtained using the spin coating method. When they examined the samples they obtained, they stated that Co-doped CuO thin films showed better photocatalytic properties than undoped and Fe-doped thin films. Tawfik *et al*. [19] have shown that the resistance of undoped and Co-doped CuO thin films prepared by using DC and AC reactive magnetron sputtering techniques decreased with some increase in the Co dopant ratio. Moreover, in other work carried out in the literature, Glass/F: SnO_2/CdS/CuO/Ag heterojunction solar cell structure was successfully fabricated using magnetron sputtering, in which CuO acted as an absorber layer. The absorption coefficient ($\alpha > 105cm^{-1}$) of this layer was found to be quite high. It was reported that the $F:SnO_2$ films were observed to be quite transparent (Tr > 90%), possessing a band gap of ~3.45eV [20]. In another study, CuO thin films with an energy band gap of 1.47eV were produced using the spin coating technique. The prepared CuO thin films were optimised by the Taguchi model, and this led to improvement in optical properties. The findings of this study suggested that CuO thin films could potentially be used as solar cell absorbers in photovoltaic devices [21].

Nowadays, simulation software has been employed to determine the solar cells' efficiency courtesy of layers constructing solar cells, which have some crucial effects. One of the most employed software in this area is SCAPS-1D. SCAPS-1D is a package program that computes Photovoltaic (PV) parameters of solar cells by employing physical parameters, such as; dielectric permittivity, energy band gap, the electron affinity of layers comprising a solar cell, thin film thickness, the work function of contacts, etc. as input data [22, 23]. Based on parameters such as the Auger electron/hole capture coefficient, operation temperature, and interfacial defect density [24], solar cells' PV parameters can be determined, and therefore, a reliable estimate can be reached on the solar cell's performance. The physical properties and phase formations of CuO thin films have been affected by changing the production conditions (such as sulphur content or partial pressure, duration and temperature) of the desulphurisation process [25]. This work aims to investigate the photovoltaic parameters that would improve the efficiency of a solar cell. Thus, the main motivation behind this work is the hope for utilising undoped and doped CuO thin film materials for photovoltaic applications and contributing to the limited current literature.

Structural, morphological and optical properties of thin films obtained have been studied by carrying out several techniques employing X-Ray diffraction (XRD), Scanning electron microscopy (SEM) and UV-Vis spectrophotometry (UV-Vis), respectively. In this work, undoped and Ag-doped CuO thin films have been produced by means of the spin coating technique. Moreover, Ag/undoped CuO and Ag-doped CuO/ZnO/AZO solar cells have been modelled, and their PV parameters have been calculated using the SCAPS simulation program.

2. EXPERIMENTAL

In order to deposit Ag-doped CuO thin films on a glass substrate by employing the spin coating technique, they were first dissolved in ethanol using 0.1M copper(II) acetate ($Cu(CH_3COO)_2 \cdot H_2O$) and 0.01M silver nitrate ($AgNO_3$). These solutions were vibrated at room temperature for 24 hours to obtain a homogeneous solution. Then, solutions attained were added to Cu solution at Ag ratios of 0 and 1% and vibrated again at room temperature for 3 hours. Prior to deposition on the glass substrate, the substrates must first be 5:1:1 H_2O, NH_3 and H_2O_2 for 15 minutes at 90°C and then 5:1:1 H_2O, H_2O_2 and HCl mixture under the same conditions to obtain a clean and homogeneous film. Then, cleaned substrates were vibrated in acetone and ethanol for 3 minutes, respectively, and after these processes, cleaned substrates were treated with distilled water and then dried under N_2 gas to remove the water from the surface. In order to obtain four different concentrations of Ag-doped CuO thin films, solutions were deposited on glass substrates for 65s in a spin coating device set at 2000rpm for a total of ten layers. Each thin film layer was preheated at 200°C for 10 minutes on a hot plate to obtain a homogeneous thin film during the deposition process. After the processes mentioned above were completed during the preparation of films, all of the films were annealed in the air for 1 hour in an oven that was gradually brought to 500°C. Rigaku Ultima III diffractometer (XRD: Cu Kα radiation, λ=1.540056Å) instrument (Rigaku, Ultima III, XRD) was employed to analyse the structural properties of films obtained. Thin films' surface properties were analysed using a scanning electron microscope device, and thin films' energy band gap and transmittance values were calculated over a wavelength range of 300-1100nm using a spectrophotometer (Shimadzu, UV-3600, UV-Vis).

3. RESULTS AND DISCUSSIONS

3.1. XRD and SEM

Ag-doped CuO thin films' structural properties were determined using XRD spectroscopy. Figure **1** shows the XRD spectrum of Ag-doped CuO thin films prepared at different concentrations (0 and 1%) by spin coating technique. Except for peaks of CuO (for example, Cu_2O or silver oxide), no peaks were observed, indicating that the films obtained were homogeneous. When the figure is examined, it is seen that there are two large peaks with a tenorite structure of polycrystalline nature, located at approximately 35.5° and 38.6° with orientations (002) and (111), respectively. In addition, d_{hkl} values of these peaks are approximately 2.52Å for 35.5° and 2.32Å for 38.6°. In addition to these two large peaks, there are also some other peaks with tenorite structures of (-202) and (022) around 48.92° and 66.06°, respectively. When the figure is examined, it is seen that the intensity of the (002) and (111) peaks are high, and peak positions for (002) remain almost the same, but there is a small change for (111).
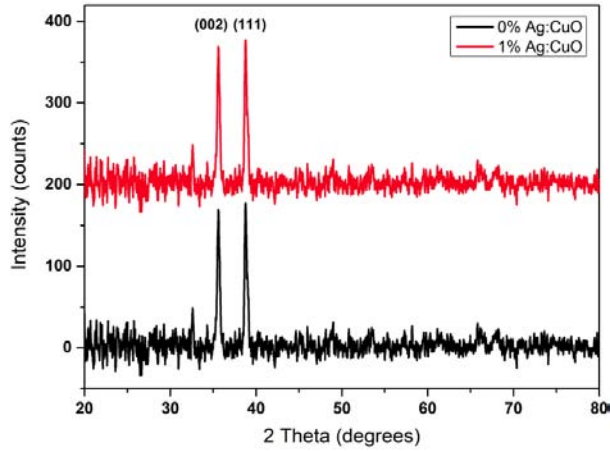
Figure 1: XRD patterns of undoped and 1% Ag doped CuO thin films.

Das ve Alford [26] stated that the position of peaks obtained in their Ag-doped CuO studies remained almost the same for (111) and changed little for (-111). The position of the peaks, full width at half maximum (FWHM), dislocation density (δ) and crystal size (D), diffraction angle (2θ) from XRD spectrum, and inter plenary distance (d) were calculated as a function of concentration and shown in Table **1**, the detailed calculations and formulas are presented elsewhere [27].

The surface morphologies of obtained thin films are very significant for analysing the surface properties of thin films. Figure **2** displays SEM images of CuO thin films with 0 and 1% Ag concentrations grown using the spin coating method.

It is seen that the films have an almost flat and homogeneous surface, although there are very few defects, such as cracks and voids, as shown in the figure. Samples obtained appear to be relatively smooth and more homogeneously dispersed with little agglomeration to the substrate used. It can be seen that there is a difference in CuO morphology as they tend to be hemispherical nanostructured films with more homogeneous distribution and small agglomeration. Jabbar stated that CuO, which he synthesised using sol-gel and chemical precipitation methods, has similar surface properties [28]. This suggests that the surface morphologies of produced CuO thin films in this study are in good agreement with previous studies.

3.2. Optical Properties of Undoped and Ag-Doped CuO Thin Film

According to the absorption spectrum represented in Figure **3a**, it can be clearly said that Ag-doped CuO thin film absorbs more photons over a spectral range from Vis to NIR regions, while it absorbs fewer photons in the UV region compared to non-doped thin films. The optical energy band gap (E_g) for the undoped CuO and Ag-doped CuO thin films can be determined by the Tauc formula (Eq. (1)):

$$\alpha h\upsilon = \beta(h\upsilon - E_g)^{1/2} \tag{1}$$

where β is an energy-independent constant and $h\upsilon$ is photon energy. As seen in the Tauc plot in Figure **3b**, direct energy band gaps (E_g) of undoped and Ag-doped CuO thin films

Table 1: XRD Data of Ag-Doped Thin Films Annealed in Air at 500°

	2θ (Degrees)	FWHM (RadianX10^{-4})	D (nm)	d (Experiment) (Å)	d (Teory) (Å)	δ (10^{14}m^2)	ε (x10^{-3})	Orientation
0% Ag:CuO	0.33	57.6	26.4	2.52	2.52	1.43	4.5	002
	0.29	50.6	30.4	2.32	2.32	1.08	3.6	111
1% Ag:CuO	0.33	57.6	26.4	2.52	2.52	1.43	4.5	002
	0.31	54.1	28.4	2.32	2.32	1.24	3.9	111
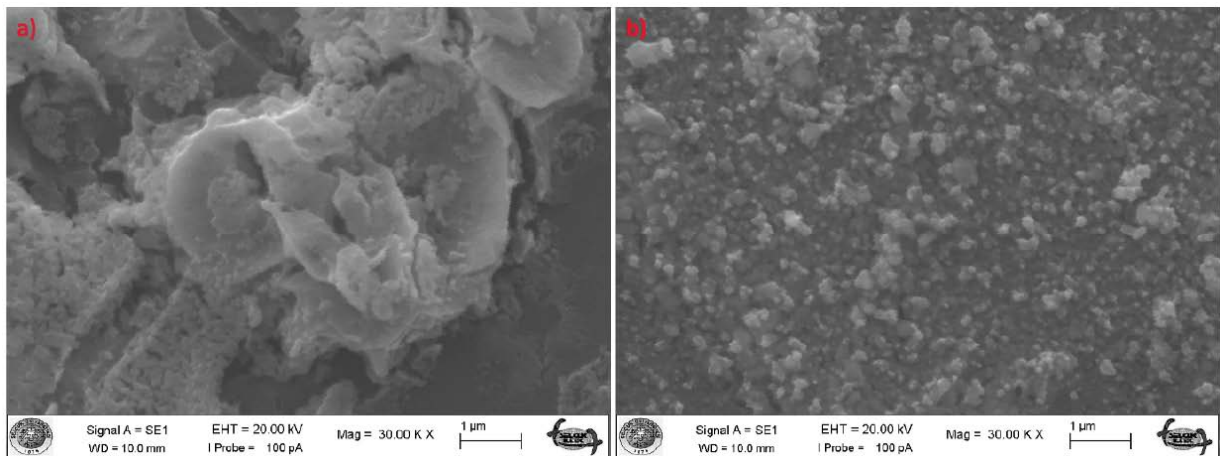
Figure 2: SEM images of undoped and 1% Ag-doped CuO thin films, respectively.
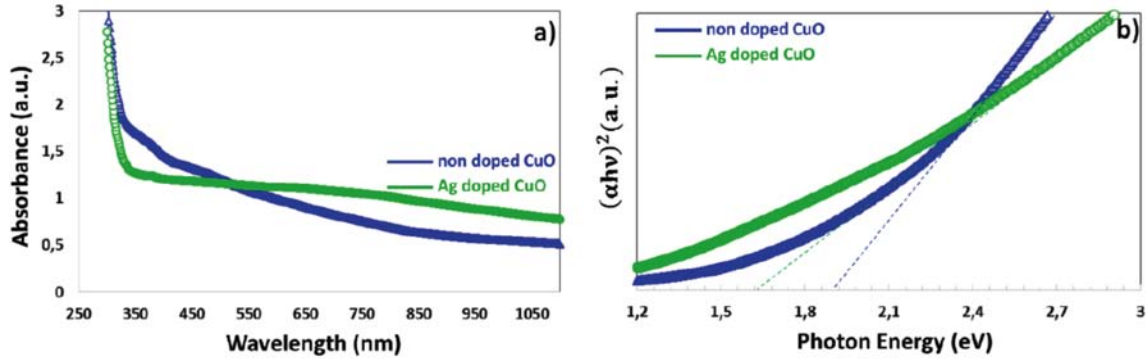
Figure 3: a) Absorbance spectrum and, **b**) Tauc Plot of non-doped and Ag-doped CuO thin films.
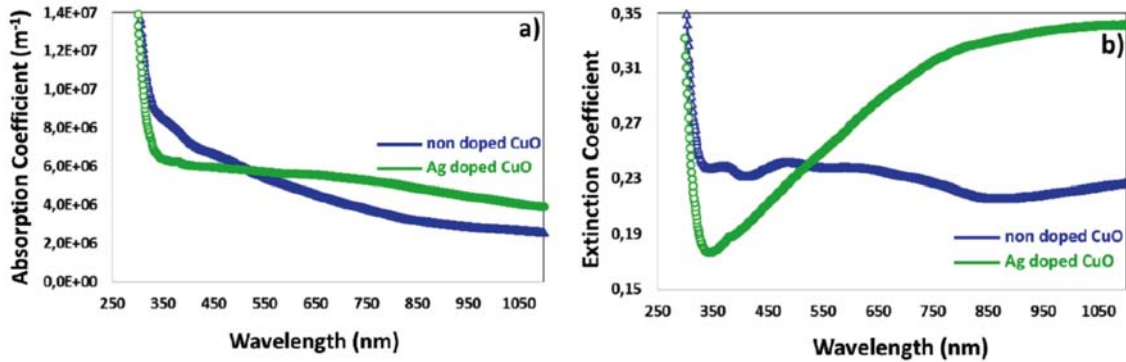
Figure 4: a) Absorption and, **b**) Extinction Coefficient spectrum of undoped and Ag-doped CuO thin films.

were calculated as 1.90eV and 1.63eV, respectively. This is because the Ag-doped CuO thin film absorbs more photons towards to NIR region; the band gap thus is lower than the undoped thin film. In addition, Ag atoms may have formed some defects at the shallow band gap level, which causes the band gap to decrease.

The absorption coefficient (α) of a thin film is calculated by Eq (2) [29, 30]:

$$\alpha = 2.303(A/T) \tag{2}$$

Where A and T are the absorption coefficient and thin film thickness, the undoped and Ag-doped CuO thin films have an average absorption coefficient of $4.10^6 m^{-1}$ and $6.10^6 m^{-1}$, respectively, in the visible region. Moreover, Ag limits the diffusion of light, causing some increase in the absorption coefficient.

The extinction coefficient (k) of a thin film is expressed by Eq. (3) [31]:

$$k = \frac{\alpha\lambda}{4\pi} \tag{3}$$

Where α is the absorbance coefficient, λ is the wavelength of the photon applied. According to Figure **4**, Ag-doped CuO thin film shows a high extinction coefficient from visible to near-infra-red regions. However, it absorbs fewer photons in the UV region, and these findings agree with data in the

absorption spectrum. The undoped CuO thin film has a more stable extinction coefficient ranging from UV to NIR region.

The refractive index (n) of light has a significant effect on the absorption and extinction of light. The refractive index of light is expressed by the following Eq. (4) using the Moss relation [32]:

$$E_g n^4 = k \tag{4}$$

Where k is a constant that has a value of 108 eV. Also, n is defined using Eq. (5) by Herve and Vandamme [32].

$$n = \sqrt{1 + \left(\frac{A}{E_g + B}\right)^2} \tag{5}$$

A and B are constants and have values of 13.6eV and 3.4eV, respectively. n (Refractive index) is calculated using Eq. (4) and (5) and is given in Table **1**. The refractive index is calculated by both relations, and it has been noticed that they exhibit good compatibility with one another. It can be emphasised that the refractive index of thin films increases with decreasing band gap. The refractive index can cause the light to play an active role in the semiconductor thin film and the formation of more photo-excited charge carriers. Therefore, a high number of charge carriers can be found in Ag-doped CuO thin films, which have a higher refractive index. The electric field is created among semiconductors' charges and provides an opportunity to define the dielectric

Table 2: **The Energy Band Gaps, Refractive Index, High-Frequency Dielectric and Static Dielectric Constants of Undoped and Ag-Doped CuO Thin Films**

Samples	E_g (eV)	Moss relation		Herve & Vandemme		Static Dielectric Constant, ε_o
		n	ε_∞	n	ε_∞	
undoped CuO	1.90	2.74	7.53	2.75	7.58	12.66
Ag doped CuO	1.63	2.85	8.13	2.88	8.31	13.49

coefficient. The dielectric coefficient can contribute to the easy charge transition in the semiconductor and supports some increments in the charge aggregation in the solar cell. Eq. (6) and Eq. (7) are used to express the high-frequency dielectric constant (ε_∞) and the static dielectric constant (ε_o), respectively:

$$\varepsilon_\infty = n^2 \tag{6}$$

$$\varepsilon_o = 18.52 - 3.08 E_g \tag{7}$$

The dielectric coefficients of thin films were found using the refractive indices calculated by Moss and Herve and Vandemme relations and are given in Table **2**.

3.3. Modelling Ag/Undoped and Ag-Doped CuO/n-Zn/AZO Solar Cells using a SCAPS-1D Simulation Program

SCAPS-1D is a package program that calculates PV parameters by using some related physical parameters of layers in heterojunction, perovskite, dye-sensitised solar cells, etc. [31, 33, 34]. In this study, in order to calculate PV parameters of undoped and Ag-doped CuO thin film solar cells using the SCAPS-1D simulation program, the thickness value, energy band gaps and absorption coefficient spectral file for the undoped and Ag-doped CuO thin films produced experimentally were used as an input for simulation program [24, 35-41]. Apart from these, the other physical parameters of layers forming Ag/undoped CuO/n-ZnO/AZO and Ag/Ag
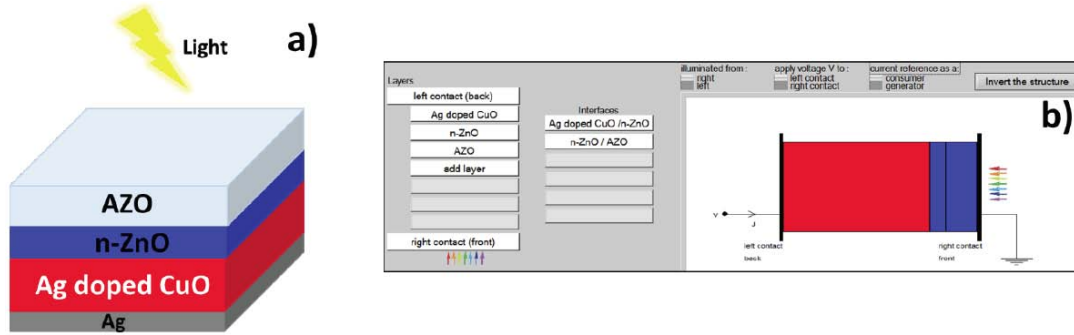
Figure 5: Ag-doped CuO solar cell diagram modelled by the SCAPS-1D simulation program.

Table 3: **The Physical Parameter of the Layer Formed the Undoped and Ag-Doped CuO Thin Film Solar Cell**

Layers	AZO [42]	ZnO [43]	CuO [41]	Ag doped CuO [24, 35-40]
Band Gap (eV)	3.3	2.4	1.90	1.63
Electron affinity (eV)	4.6	4.6	4.2	4.4
Dielectric permittivity (relative)	9	9	12.66	13.49
CB effective density of states (cm^{-3})	2.20×10^{18}	1.80×10^{18}	2.20×10^{19}	2.20×10^{19}
VB effective density of states (cm^{-3})	1.80×10^{19}	2.40×10^{19}	5.50×10^{20}	5.50×10^{20}
Electron/Hole thermal velocity (cm/s)	1.00×10^{7}	1.00×10^{7}	1.00×10^{7}	1.00×10^{7}
Electron/Hole mobility (cm^2/Vs)	100/25	100/25	100/25	100/20
Shallow donor density (cm^{-3})	1.00×10^{20}	1.00×10^{18}	0	0
Shallow acceptor density (cm^{-3})	0	0	1.00×10^{16}	6.5×10^{16}
Thickness (nm)	100	50	460	460
Contacts			Back Contact (Ag) [31]	
Metalwork function(eV)			4.66	
Surface recombination velocity of electrons (cm/s)			1×10^{7}	
Surface recombination velocity of holes (cm/s)			1×10^{5}	

Candan et al.

doped CuO/n-ZnO/AZO solar cells (shown in Figure **5**) that given in Table **3**.

3.3.1. The Energy Band Diagram and the Generation Rate of the Undoped and Ag-Doped CuO Solar Cells

In-band diagrams given in Figure **6**, it can easily be seen and concluded that there is a slightly different band alignment according to energy band gaps of semiconductors formed in undoped and Ag-doped CuO solar cells. A Schottky contact and non-ohmic behaviour are observed in the back contact region for p-type semiconductors in Ag-doped CuO thin-film solar cells [44]. In this region, the charges undergo recombination, negatively affecting the charge aggregation and decreasing V_{oc} value. Both solar cells formed a cliff-like band alignment. However, band bending is more pronounced in the depletion region of Ag-doped CuO solar cells. In this case, a non-ideal conduction band offset could occur between Ag-doped CuO and n-ZnO semiconductors. Thus, electrons and holes can recombine in the depletion region, undesirably affecting the PV performance of solar cells [45].

The generation rate-position characteristics of undoped and Ag-doped CuO solar cells are demonstrated in Figure **7**. Since the light comes directly from the AZO layer, photo-excited charge carriers with a maximum value of 1.49×10^{22} $1/cm^3$.s were formed in an undoped CuO absorber semiconductor close to the depletion region in a solar cell (at 0.465 μm position) [46, 47]. Since the diffusion of light towards the rear contact region decreases, the number of photo-excited charge carriers decreases towards this region.

The generation rate of photo-excited charge carriers at the back side of undoped CuO thin film is 2.85×10^{19} $1/cm^3$.s (illustrated in Figure **5a**). However, as ZnO and AZO semiconductors are transparent semiconductors, the generation rate in these semiconductors is very low. Since Ag-doped CuO thin film has a high absorption coefficient over a spectral region from Vis to NIR region, the generation rate in the 0.465 μm region of this thin film is about 1.51×10^{25} $1/cm^3$.s (Figure **5b**). The generation rate in the back region of Ag-doped CuO thin film is about 2.89×10^{19} $1/cm^3$.s. Due to the high absorption coefficient of Ag-doped CuO thin film, the number of high photo-excited charges fashioned in the depletion region is quite high compared to a non-doped thin film.

3.3.2. The Effect of the Acceptor Density of (N_a) of Ag-Doped CuO thin Film Solar Cell

Figure **8** illustrates the effect of the acceptor density on PV parameters of Ag-doped CuO thin film. N_a value represents acceptor defects which express hole concentrations that increase the p-type conductivity of absorber layers. The higher hole concentration reduces the saturation current. Also, as a result of doping, the depletion region is narrowed where the electrical field increases and charge aggregation increases. Therefore, V_{oc} and J_{sc} values increase as N_a increases, and this finding is in good agreement with the literature [48, 49]. If the N_a value is less than 1.0×10^{16} cm^{-3} or greater than 2.0×10^{17} cm^{-3}, it can negatively affect the efficiency of the solar cell. Thus, when the hole concentration
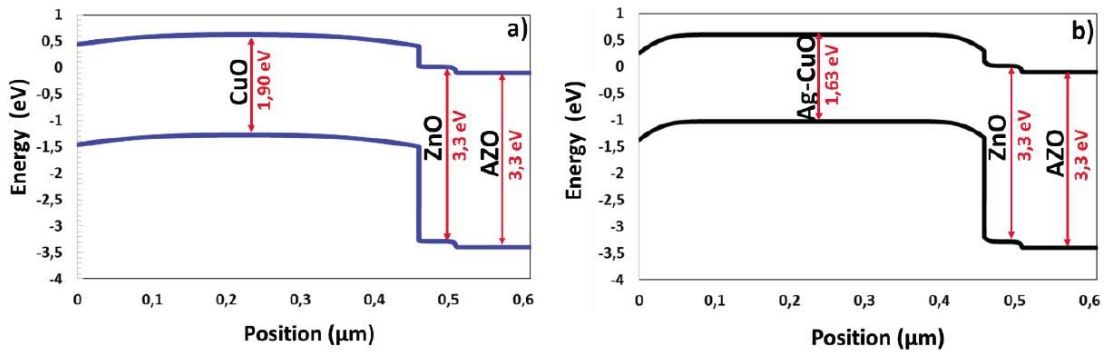
Figure 6: The energy band diagram of undoped and Ag-doped CuO thin film solar cells.
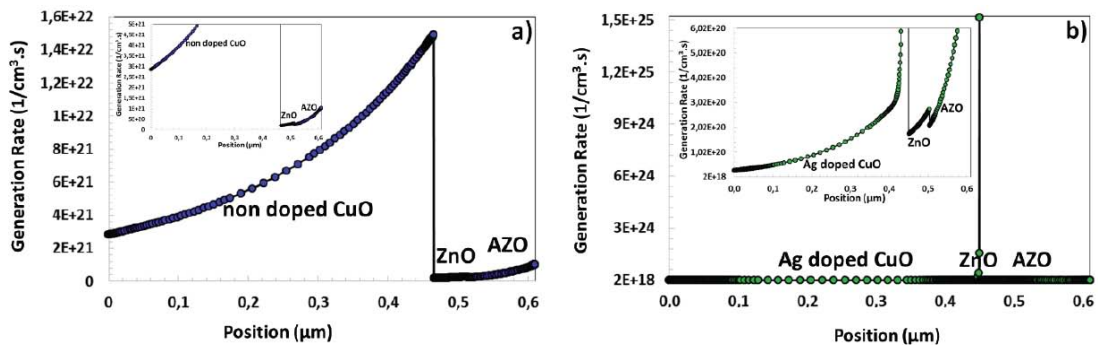
Figure 7: The generation rate-position characteristics of **a**) undoped and **b**) Ag-doped CuO thin film solar cells.
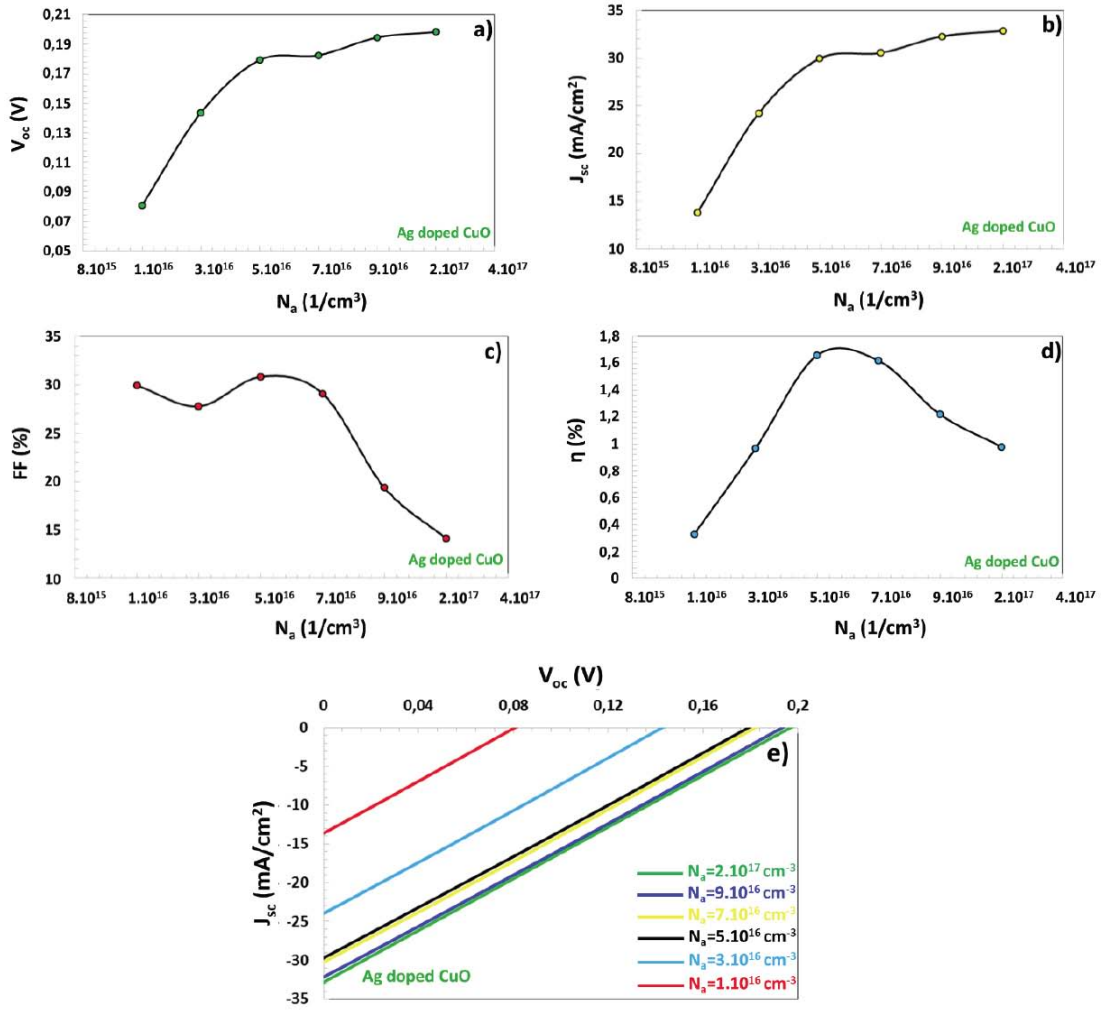
Figure 8: The effect of the acceptor density (N_a) on photovoltaic parameters of Ag-doped CuO thin film solar cell.

increases, the diffusion length of the minority charge carriers is reduced, resulting in some lower efficiency, as stated by Meher *et al.* [50]. V_{oc}, J_{sc}, and η values have increased from 0.08V to 0.1986V, from 13.80mA/cm^2 to 32.87mA/cm^2 and from 0.33% to 0.98%, respectively, FF value has decreased from 29.94% to 14.09% while N_a value enhanced from 1.10^{16}cm^{-3} to 2.10^{17}cm^{-3} according to Figure **5**. However, Ag doped CuO solar cell exhibited the highest efficiency of 1.66%, for Na=6.5x10^{16} cm^{-3}. Corresponding to this N_a value, V_{oc}, J_{sc}, and FF values are 0.179V, 29.95mA/cm^2, and 30.83%, respectively.

3.3.3. The Effect of the Interface Defect Density (N_t) on Undoped and Ag-Doped CuO Thin Film Solar Cells

Figures **9** and **10** show the effects of N_t value on PV parameters of the undoped and Ag-doped CuO thin film solar cells, respectively. Defects between undoped/Ag-doped CuO and n-ZnO semiconductors behave as charge carriers at recombination points. These flaws are situated close to the band edges contributing to the recombination of Shockley-Read Hall (SHR) as the carrier is possibly to reappear back in the shallow levels of respective bands [50]. This recombination adversely affects solar cell performance by

reducing charge aggregation at the depletion region. In solar cells based on undoped CuO thin films, there was no change in PV parameters at N_t values smaller than 10^9 cm^{-3}, but below this N_t value, the magnitude of J_{sc}, V_{oc}, FF and η parameters have decreased [51-53]. This change started beyond the value of N_t=10^{10}cm^{-3}. Therefore, N_t=10^{9}cm^{-3} and N_t=10^{10}cm^{-3} interfacial defect densities indicate the downstream break point in efficiency for undoped and Ag-doped CuO solar cells, respectively. When the N_t value is increased from 10^{9}cm^{-3} to 10^{14}cm^{-3}, V_{oc}, J_{sc}, FF and η values decrease from 0.267V to 0.100V, from 33.52mA/cm^2 to 16.55mA/cm^2, from 35.24% to 24.9% and from 3.16% to 0.41% for the undoped CuO thin film solar cell, respectively. For Ag-doped CuO solar cells, V_{oc}, J_{sc}, FF and η values decrease from 0.179V to 0.174V, from 29.03mA/cm^2 to 17.06mA/cm^2, from 30.83% to 19.41% and from 1.66% to 0.58%, respectively, when N_t value is increased from 10^{10}cm^{-3} to 10^{14}cm^{-3}. If the performances of two solar cells are evaluated, it has been observed that Ag doping negatively affects the solar cell's efficiency. As can be seen from the band diagrams in Figure **3b**, the non-ideal conduction band offset between the Ag-doped CuO
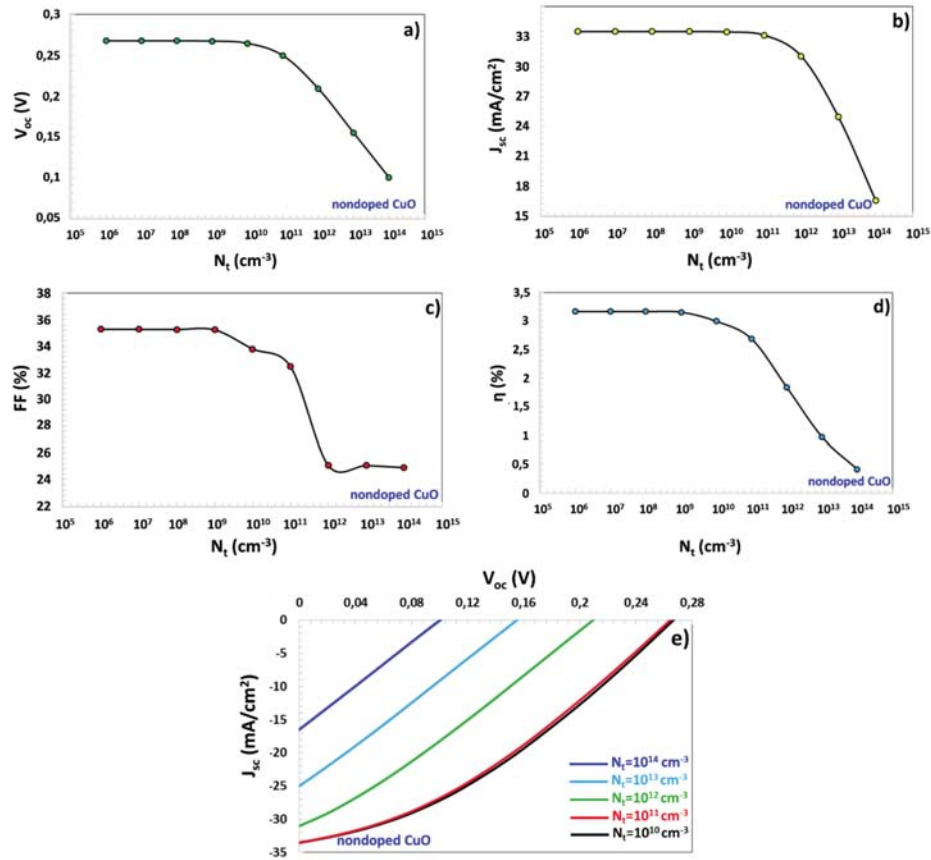
Figure 9: The effect of the interface defect density (N_t) on photovoltaic parameters of Ag-doped CuO thin film solar cell.
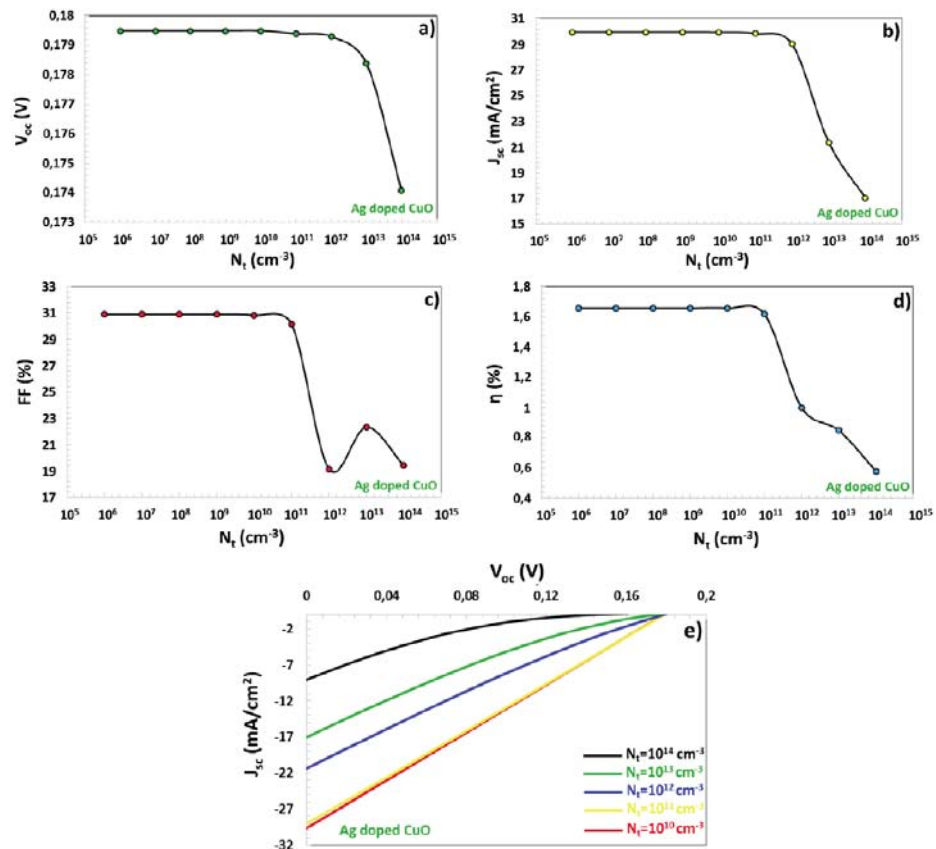
Figure 10: The effect of the interface defect density (N_t) on photovoltaic parameters of Ag-doped CuO thin film solar cell.
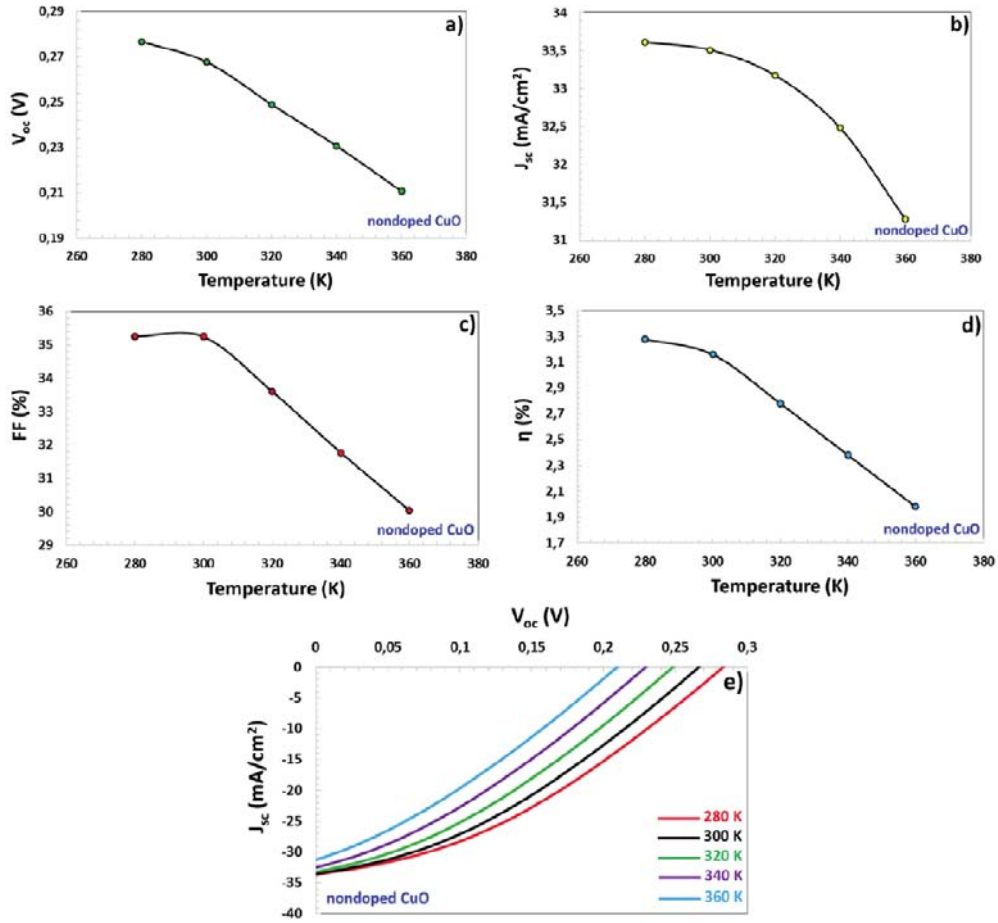
Figure 11: The effect of the operating temperature on undoped CuO thin film solar cell's photovoltaic parameters.

semiconductor with 1.63eV band and ZnO semiconductor with 3.3eV band gap causes recombination in the depletion region and adversely affects the efficiency. Moreover, the Ag doping element may have caused SHR recombination.

3.3.4. The Effect of the Operating Temperature on the Undoped and Ag-Doped CuO Thin Film Solar Cell

The climatic conditions of the place where solar cells are located have a large influence on the efficiency of solar cells. For observing the effect of temperature on the solar cell, some change in PV parameters of undoped and Ag-doped CuO solar cells between 280 and 360°K temperature was examined, as shown in Figures **11** and **12**. It has been obtained that as the temperature increases, the performance of solar cells deteriorates. As the studies revealed, at high temperatures, the kinetic energy of electrons upsurges and their motion becomes unstable. These unstable electrons undergo recombination at trap points [54, 55]. Other studies suggest that at high temperatures, the band gap becomes narrower, band alignment is disrupted, and recombination occurs due to undesired charge transitions [42, 56-58]. In an undoped CuO solar cell, V_{oc}, FF and n values decrease almost linearly, and Jsc shows some parabolic decrease. But in Ag-doped CuO solar cells, V_{oc} and J_{sc} increase almost linearly, and some fluctuations in FF and η values were

observed. Changes in the maximum output current and maximum voltage value can cause these fluctuations. As a result, V_{oc}= 0.267V, J_{sc}=33.51mA/cm^2, FF=35.25%, and η=3.16% values are values for an ideal non-doped solar cell at room temperature, while V_{oc}= 0.1795V, J_{sc}=29.95mA/cm^2, FF=30.83% and η=1.66% to Ag-doped CuO solar cell with the highest efficiency at room temperature. Accordingly, it was concluded that Ag doping negatively affects the efficiency of the CuO solar cell in Figure **6f**.

4. CONCLUSIONS

Undoped and Ag-doped CuO thin films have been manufactured courtesy of the spin coating technique. Thin films' structural, morphological and optical properties investigated in this work have been carried out by employing X-Ray diffraction (XRD), Scanning electron microscopy (SEM), and UV-Vis-NIR spectrophotometry (UV-Vis-NIR), respectively. Structural analysis suggests that thin films have polycrystalline nature with two preferred orientations of (002) and (111). The morphology of films is homogeneous based on SEM images. Ag-doped CuO thin film absorbs more photons from Vis to the NIR region, while it absorbs fewer photons in the UV region compared to non-doped thin films, based on the absorption spectrum.
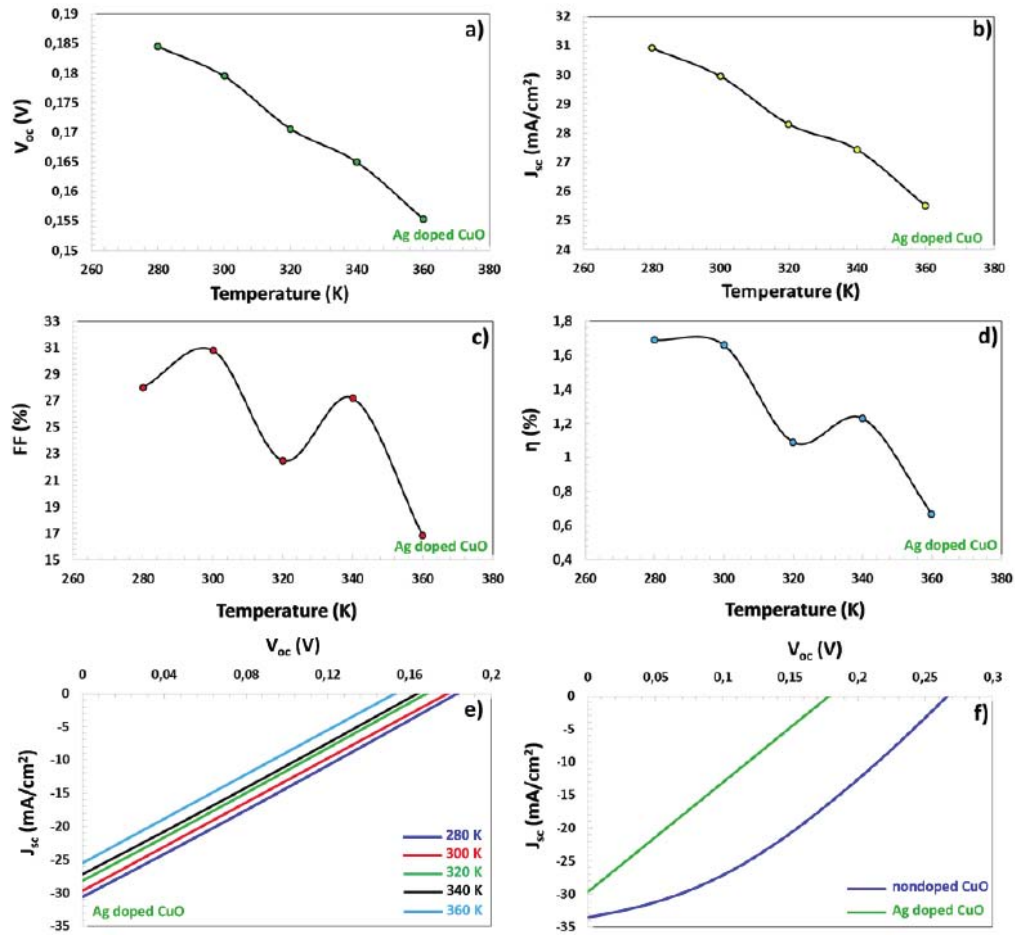
Figure 12: The effect of the operating temperature on photovoltaic parameters of Ag-doped CuO thin film solar cell.

- The band gaps of undoped and Ag-doped CuO thin films have been calculated to be 1.90eV and 1.63eV, respectively.

- Ag-doped CuO thin film has higher absorption and extinction coefficients in the visible region compared to undoped CuO thin film.

- Using the SCAPS package program, undoped and Ag-doped CuO solar cells have been modelled, and their PV parameters have been calculated.

- While the maximum charge generation at 1.49×10^{22} $1/cm^3$.s occurs in undoped CuO solar cells, the highest charge formation in Ag-doped CuO solar cells is 1.51×10^{25} $1/cm^3$.s.

- While N_a raised from 1.10^{16} to 2.10^{17} cm^{-3} in Ag-doped CuO solar cell, V_{oc}, J_{sc} and FF values increased, but the highest efficiency was reached for $N_a=6, 5.10^{16}$ cm^{-3}.

- PV performances of undoped and Ag-doped CuO solar cells started to deteriorate after 10^9 cm^{-3} and 10^{10} cm^{-3} N_t values, respectively.

- The purpose of this work was to investigate the photovoltaic parameters that would improve the efficiency of a solar cell.

- It has also been pointed out and concluded that the operating temperature for solar cells negatively affects the efficiency of both types of solar cells. As a result, Ag doping has deteriorated the performance of CuO solar cells.

- Therefore, these parameters could be investigated experimentally for possible future photovoltaic applications.

ACKNOWLEDGEMENTS

- Dicle University Scientific Research Project (BAP) Coordination office

COMPETING INTERESTS

The authors have no relevant financial or non-financial interests to disclose.

REFERENCES

[1] Deng H, Li H-r, Wang F, Yuan C-x, Liu S, Wang P, *et al*. A high sensitive and low detection limit of formaldehyde gas sensor based on hierarchical flower-like CuO nanostructure fabricated by sol-gel method. J Mater Sci Mater Electron 2016; 27(7): 6766-72.
https://doi.org/10.1007/s10854-016-4626-y

[2] Sanal K, Vikas L, Jayaraj M. Room temperature deposited transparent p-channel CuO thin film transistors. Appl Surf Sci 2014; 297: 153-7.
https://doi.org/10.1016/j.apsusc.2014.01.109

[3] Chaudhary YS, Agrawal A, Shrivastav R, Satsangi VR, Dass S. A study on the photo-electrochemical properties of copper oxide thin films. Int J Hydrog Energy 2004; 29(2): 131-4.
https://doi.org/10.1016/S0360-3199(03)00109-5

[4] Bhaumik A, Haque A, Karnati P, Taufique M, Patel R, Ghosh K. Copper oxide based nanostructures for improved solar cell efficiency. Thin Solid Films 2014; 572: 126-33.
https://doi.org/10.1016/j.tsf.2014.09.056

[5] Kang BS, Ahn SE, Lee MJ, Stefanovich G, Kim KH, Xianyu WX, *et al*. High-Current-Density CuO x/InZnOx Thin-Film Diodes for Cross-Point Memory Applications. Adv Mater 2008; 20(16): 3066-9.
https://doi.org/10.1002/adma.200702932

[6] Zhang Q, Zhang K, Xu D, Yang G, Huang H, Nie F, *et al*. CuO nanostructures: synthesis, characterisation, growth mechanisms, fundamental properties, and applications. Prog Mater Sci 2014; 60: 208-337.
https://doi.org/10.1016/j.pmatsci.2013.09.003

[7] Baturay S, Candan I, Ozaydın C. Structural, optical, and electrical characterisations of Cr-doped CuO thin films. J Mater Sci Mater Electron 2022; 33(9): 7275-87.
https://doi.org/10.1007/s10854-022-07918-2

[8] Morales J, Sánchez L, Martín F, Ramos-Barrado JR, Sánchez M. Nanostructured CuO thin film electrodes prepared by spray pyrolysis: a simple method for enhancing the electrochemical performance of CuO in lithium cells. Electrochim Acta 2004; 49(26): 4589-97.
https://doi.org/10.1016/j.electacta.2004.05.012

[9] Menazea A, Mostafa AM. Ag-doped CuO thin film prepared via pulsed laser deposition for 4-nitrophenol degradation. J Environ Chem Eng 2020; 8(5): 104104.
https://doi.org/10.1016/j.jece.2020.104104

[10] Jundale D, Joshi P, Sen S, Patil V. Nanocrystalline CuO thin films: synthesis, microstructural and optoelectronic properties. J Mater Sci Mater Electron 2012; 23(8): 1492-9.
https://doi.org/10.1007/s10854-011-0616-2

[11] Dahrul M, Alatas H. Preparation and optical properties study of CuO thin film as applied solar cell on LAPAN-IPB Satellite. Procedia Environ Sci 2016; 33: 661-7.
https://doi.org/10.1016/j.proenv.2016.03.121

[12] Valladares LDLS, Salinas DH, Dominguez AB, Najarro DA, Khondaker S, Mitrelias T, *et al*. Crystallisation and electrical resistivity of Cu2O and CuO obtained by thermal oxidation of Cu thin films on SiO2/Si substrates. Thin Solid Films 2012; 520(20): 6368-74.
https://doi.org/10.1016/j.tsf.2012.06.043

[13] Al-Kuhaili M. Characterization of copper oxide thin films deposited by the thermal evaporation of cuprous oxide (Cu2O). Vacuum 2008; 82(6): 623-9.
https://doi.org/10.1016/j.vacuum.2007.10.004

[14] Terasako T, Ohmae K, Yamane M, Shirakata S. Carrier transport in undoped CdO films grown by atmospheric-pressure chemical vapor deposition. Thin Solid Films 2014; 572: 20-7.
https://doi.org/10.1016/j.tsf.2014.07.061

[15] Singh R, Yadav L, Shweta T. Effect of annealing time on the structural and optical properties of n-CuO thin films deposited by sol-gel spin coating technique and its application in n-CuO/p-Si heterojunction diode. Thin Solid Films 2019; 685: 195-203.
https://doi.org/10.1016/j.tsf.2019.06.026

[16] Masudy-Panah S, Radhakrishnan K, Tan HR, Yi R, Wong TI, Dalapati GK. Titanium-doped cupric oxide for photovoltaic application. Sol Energy Mater Sol Cells 2015; 140: 266-74.
https://doi.org/10.1016/j.solmat.2015.04.024

[17] Basith NM, Vijaya JJ, Kennedy LJ, Bououdina M. Structural, optical and room-temperature ferromagnetic properties of Fe-doped CuO nanostructures. Phys E: Low-Dimens Syst Nanostruct 2013; 53: 193-9.
https://doi.org/10.1016/j.physe.2013.05.009

[18] El Sayed A, Shaban M. Structural, optical and photocatalytic properties of Fe and (Co, Fe) co-doped copper oxide spin-coated films. Spectrochim. Acta A Mol 2015; 149: 638-46.
https://doi.org/10.1016/j.saa.2015.05.010

[19] Tawfik WZ, Khalifa ZS, Abdel-Wahab MS, Hammad AH. Sputtered cobalt-doped CuO nanostructured thin films for photoconductive sensors. J Mater Sci Mater Electron 2019; 30(2): 1275-81.
https://doi.org/10.1007/s10854-018-0395-0

[20] Dolai S, Dey R, Hussain S, Bhar R, Pal AK. Photovoltaic properties of F: SnO2/CdS/CuO/Ag heterojunction solar cell. Mater Res Bull 2019; 109: 1-9.
https://doi.org/10.1016/j.materresbull.2018.09.022

[21] Absike H, Essalhi Z, Labrim H, Hartiti B, Baaalla N, Tahiri M, *et al*. Synthesis of CuO thin films based on Taguchi design for solar absorber. Opt Mater 2021; 118: 111224.
https://doi.org/10.1016/j.optmat.2021.111224

[22] Piñón Reyes AC, Ambrosio Lázaro RC, Monfil Leyva K, Luna López JA, Flores Méndez J, Heredia Jiménez AH, *et al*. Study of a lead-free perovskite solar cell using CZTS as HTL to achieve a 20% PCE by SCAPS-1D simulation. Micromachines 2021; 12(12): 1508.
https://doi.org/10.3390/mi12121508

[23] AlZoubi T, Moghrabi A, Moustafa M, Yasin S. Efficiency boost of CZTS solar cells based on double-absorber architecture: Device modeling and analysis. Sol Energy 2021; 225: 44-52.
https://doi.org/10.1016/j.solener.2021.07.012

[24] Houimi A, Gezgin SY, Mercimek B, Kılıç HŞ. Numerical analysis of CZTS/n-Si solar cells using SCAPS-1D. A comparative study between experimental and calculated outputs. Opt Mater 2021; 121: 111544.
https://doi.org/10.1016/j.optmat.2021.111544

[25] Pallavolu MR, Reddy VRM, Pejjai B, Jeong D-s, Park C. Effect of sulfurisation temperature on the phase purity of Cu2SnS3 thin films deposited via high vacuum sulfurisation. Appl Surf Sci 2018; 462: 641-8.
https://doi.org/10.1016/j.apsusc.2018.08.112

[26] Das S, Alford T. Structural and optical properties of Ag-doped copper oxide thin films on polyethylene napthalate substrate prepared by low-temperature microwave annealing. J Appl Phys 2013; 113(24): 244905.
https://doi.org/10.1063/1.4812584

[27] Baturay Ş, Candan İ. Structural, Optical and Morphological Properties of Ag Doped CuO Thin Films Produced by Spin Coating Method. https://dergiparkorgtr/en/pub/yyufbed 2022.
https://doi.org/10.21203/rs.3.rs-1118403/v1

[28] Jabbar SM. Synthesis of CuO nanostructure via sol-gel and precipitation chemical methods. Al-Khawarizmi Eng J 2016; 12(4): 126-31.
https://doi.org/10.22153/kej.2016.07.001

[29] Mustafa FA. Optical properties of NaI doped polyvinyl alcohol films. Phys Sci Int J 2013; 1(1): 1-9.
https://doi.org/10.1155/2013/897043

[30] Antar E. Effect of γ-ray on optical characteristics of dyed PVA films. J Radiat Res Appl Sci 2014; 7(1): 129-34.
https://doi.org/10.1016/j.jrras.2014.01.002

[31] Gezgin SY. Modelling and investigation of the electrical properties of CIGS/n-Si heterojunction solar cells. Opt Mater 2022; 131: 112738.
https://doi.org/10.1016/j.optmat.2022.112738

[32] Jahan N, Kabir H, Taha H, Hossain MK, Rahman MM, Bashar M, *et al*. A holistic approach to optical characterisations of vacuum deposited Cu2ZnSnS4 thin film coatings for solar absorbing layers. J Alloys Compd 2021; 859: 157830.
https://doi.org/10.1016/j.jallcom.2020.157830

[33] Burgelman M, Decock K, Niemegeers A, Verschraegen J, Degrave S. SCAPS manual. February 2016.

[34] Tripathi S, Lohia P, Dwivedi D. Contribution to sustainable and environmental friendly non-toxic CZTS solar cell with an innovative hybrid buffer layer. Sol Energy 2020; 204: 748-60.
https://doi.org/10.1016/j.solener.2020.05.033

[35] Jamil M, Amami M, Ali A, Mahmood K, Amin N. Numerical modeling of AZTS as buffer layer in CZTS solar cells with back surface field for the improvement of cell performance. Sol Energy 2022; 231: 41-6.
https://doi.org/10.1016/j.solener.2021.11.025

[36] Mishra SK, Padhy S, Singh UP. Silver incorporated bilayer Kesterite solar cell for enhanced device performance: A numerical study. Sol Energy 2022; 233: 1-10.
https://doi.org/10.1016/j.solener.2022.01.021

[37] Darvishzadeh P, Sohrabpoor H, Gorji NE. Numerical device simulation of carbon nanotube contacted CZTS solar cells. Opt Quantum Electron 2016; 48(10): 480.
https://doi.org/10.1007/s11082-016-0741-5

[38] Tousif MN, Mohammad S, Ferdous A, Hoque MA. Investigation of Different Materials as Buffer Layer in CZTS Solar Cells Using SCAPS. J Clean Energy Technol 2018; 6(4): 293-6.
https://doi.org/10.18178/JOCET.2018.6.4.477

[39] Frisk C, Ericson T, Li S-Y, Szaniawski P, Olsson J, Platzer-Björkman C. Combining strong interface recombination with bandgap narrowing and short diffusion length in Cu2ZnSnS4 device modeling. Sol Energy Mater Sol Cells 2016; 144: 364-70.
https://doi.org/10.1016/j.solmat.2015.09.019

[40] Haddout A, Fahoume M, Qachaou A, Raidou A, Lharch M, Elharfaoui N. Influence of composition ratio on the performances of kesterite solar cell with double CZTS layers—A numerical approach. Sol Energy 2019; 189: 491-502.
https://doi.org/10.1016/j.solener.2019.07.098

[41] Lam ND. Modelling and numerical analysis of ZnO/CuO/Cu2O heterojunction solar cell using SCAPS. Eng Res Express 2020; 2(2): 025033.
https://doi.org/10.1088/2631-8695/ab9716

[42] Adewoyin AD, Olopade MA, Oyebola OO, Chendo MA. Development of CZTGS/CZTS tandem thin film solar cell using SCAPS-1D. Optik 2019; 176: 132-42.
https://doi.org/10.1016/j.ijleo.2018.09.033

[43] AlZoubi T, Moustafa M. Numerical optimisation of absorber and CdS buffer layers in CIGS solar cells using SCAPS. Int J Smart Grid Clean Energy 2019; 8: 291-8.
https://doi.org/10.12720/sgce.8.3.291-298

[44] Hunter H. Simultaneous Ohmic Contacts to n and p-type Silicon Carbide for Future Electric Vehicles 2020.

[45] Rahman MA. Performance analysis of WSe2-based bifacial solar cells with different electron transport and hole transport materials by SCAPS-1D. Heliyon 2022; 8(6): e09800.
https://doi.org/10.1016/j.heliyon.2022.e09800

[46] Niane D, Diagne O, Ehemba AK, Soce MM, Dieng M. Generation and Recombination of a CIGSe Solar Cell under the Influence of the Thickness of a Potassium Fluoride (KF) Layer. Am Mater Sci Eng 2018; 6(2): 26-30.

[47] Abderrezek M, Djeghlal ME. Contribution to improve the performances of Cu2ZnSnS4 thin-film solar cells via a back surface field layer. Optik 2019; 181: 220-30.
https://doi.org/10.1016/j.ijleo.2018.12.048

[48] Djinkwi Wanda M, Ouédraogo S, Tchoffo F, Zougmoré F, Ndjaka J. Numerical investigations and analysis of Cu2ZnSnS4 based solar cells by SCAPS-1D. Int J Photoenergy 2016; 2016.
https://doi.org/10.1155/2016/2152018

[49] Abd El Halim B, Mahfoud A, Elamine DM. Numerical analysis of potential buffer layer for Cu2ZnSnS4 (CZTS) solar cells. Optik 2020; 204: 164155.
https://doi.org/10.1016/j.ijleo.2019.164155

[50] Meher S, Balakrishnan L, Alex Z. Analysis of Cu2ZnSnS4/CdS based photovoltaic cell: a numerical simulation approach. Superlattices Microstruct 2016; 100: 703-22.
https://doi.org/10.1016/j.spmi.2016.10.028

[51] Elhmaidi ZO, Pandiyan R, Abd-Lefdil M, El Khakani MA, editors. Pulsed laser deposition of CZTS thin films, their thermal annealing and integration into n-Si/CZTS photovoltaic devices 2016 International Renewable and Sustainable Energy Conference (IRSEC); 2016: IEEE.
https://doi.org/10.1109/IRSEC.2016.7983988

[52] Peksu E, Karaagac H. A third-generation solar cell based on wet-chemically etched Si nanowires and sol-gel derived Cu2ZnSnS4 thin films. J Alloys Compd 2019; 774: 1117-22.
https://doi.org/10.1016/j.jallcom.2018.10.012

[53] Gupta GK, Dixit A. Simulation studies of CZT (S, Se) single and tandem junction solar cells towards possibilities for higher efficiencies up to 22%. arXiv preprint arXiv: 180108498 2018.

[54] Tchognia JHN, Hartiti B, Ndjaka J-M, Ridah A, Thevenin P. Performances des cellules solaires à base de Cu2ZnSnS4 (CZTS): Une analyse par simulations numériques via le simulateur SCAPS. Afr Sci 2015; 11(4): 16-23.

[55] Padhy S, Mannu R, Singh UP. Graded band gap structure of kesterite material using bilayer of CZTS and CZTSe for enhanced performance: A numerical approach. Sol Energy 2021; 216: 601-9.
https://doi.org/10.1016/j.solener.2021.01.057

[56] Roy P, Tiwari S, Khare A. An investigation on the influence of temperature variation on the performance of tin (Sn) based perovskite solar cells using various transport layers and absorber layers. Results in Optics 2021; 4: 100083.
https://doi.org/10.1016/j.rio.2021.100083

[57] Abderrezek M, Fathi M, Djahli F. Comparative study of temperature effect on thin film solar cells 2018.

[58] Zhang H, Cheng S, Yu J, Zhou H, Jia H. Prospects of Zn (O, S) as an alternative buffer layer for Cu2ZnSnS4 thin-film solar cells from numerical simulation. Micro Nano Lett 2016; 11(7): 386-90.
https://doi.org/10.1049/mnl.2016.0130